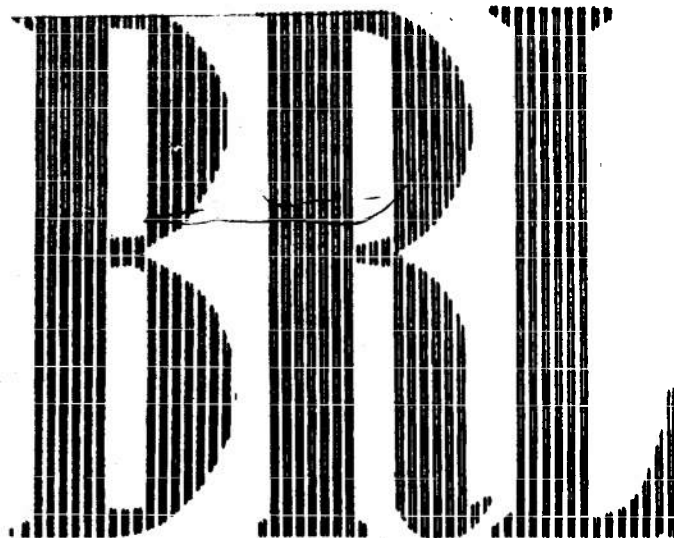


LA



REPORT NO. 1159  
DECEMBER 1961

DETONATION PROPERTIES OF PENTOLITE

TECHNICAL REPORTS SECTION  
STINFO BRANCH  
BLDG. 305

Ralph E. Shear

Department of the Army Project No. 503-04-002  
Ordnance Management Structure Code No. 5010.11.815  
**BALLISTIC RESEARCH LABORATORIES**



**ABERDEEN PROVING GROUND, MARYLAND**

ASTIA AVAILABILITY NOTICE

Qualified requestors may obtain copies of this report from ASTIA.

B A L L I S T I C   R E S E A R C H   L A B O R A T O R I E S

REPORT NO. 1159

DECEMBER 1961

DETONATION PROPERTIES OF PENTOLITE

Ralph E. Shear

Terminal Ballistics Laboratory

TECHNICAL REPORTS SECTION 7  
STEEL BRANCH  
11-22-61

Department of the Army Project No. 503-04-002  
Ordnance Management Structure Code No. 5010.11.815

A B E R D E E N   P R O V I N G   G R O U N D ,   M A R Y L A N D

BALLISTIC RESEARCH LABORATORIES

REPORT NO. 1159

REShear/plg  
Aberdeen Proving Ground, Md.  
December 1961

DETONATION PROPERTIES OF PENTOLITE

ABSTRACT

The hydrodynamic theory of detonation has been applied to determine the detonation velocity, pressure, and product composition and the isentropic expansion of the explosion products of pentolite. Hydrodynamic principles were applied to determine the initial pressure of the shock formed in air after completion of the detonation and to calculate the pressure and velocity distribution behind the detonation wave.

Page intentionally blank

Page intentionally blank

Page intentionally blank

# TABLE OF CONTENTS

	Page
ABSTRACT . . . . .	3
SYMBOLS . . . . .	7
INTRODUCTION . . . . .	9
CONDITIONS AT THE DETONATION FRONT . . . . .	10
EQUATION OF STATE . . . . .	11
CONDITIONS FOR THERMODYNAMIC EQUILIBRIUM . . . . .	13
ISENTROPIC EXPANSION OF THE EXPLOSION PRODUCTS . . . . .	17
CALCULATION OF THE INITIAL SHOCK PRESSURE IN AIR . . . . .	19
PRESSURE AND VELOCITY DISTRIBUTION BEHIND PLANE AND SPHERICAL DETONATION FRONTS . . . . .	20
CONCLUSION . . . . .	24
ACKNOWLEDGEMENT . . . . .	24
REFERENCES . . . . .	25
TABLE 1 HEATS OF FORMATION . . . . .	26
TABLE 2 COVOLUME CONSTANTS . . . . .	27
TABLE 3 IDEAL INTERNAL ENERGIES RELATIVE TO 300°K . . . . .	28
TABLE 3a IDEAL INTERNAL ENERGIES AT 300°K. . . . .	29
TABLE 4 IDEAL ENTROPIES (NON-DIMENSIONAL) . . . . .	30
TABLE 5 EQUILIBRIUM CONSTANTS . . . . .	31
TABLE 6 THERMODYNAMIC PROPERTIES OF THE EXPLOSION PRODUCTS DURING ISENTROPIC EXPANSION OF THE WAVE FRONT IN PENTOLITE AT A LOADING DENSITY OF 1.65 g/cm <sup>3</sup> . . . . .	32
TABLE 6a TEMPERATURE, VOLUME AND NUMBER OF MOLES/250g PENTOLITE OF EACH EXPANSION PRODUCT DURING ISENTROPIC EXPANSION OF THE WAVE FRONT IN PENTOLITE . . . . .	33
TABLE 7 FLOW PROPERTIES BEHIND A SPHERICAL DETONATION WAVE IN PENTOLITE AT A LOADING DENSITY OF 1.65 g/cm <sup>3</sup> . . . . .	34
TABLE 8 FLOW PROPERTIES BEHIND A PLANE DETONATION WAVE IN PENTOLITE AT A LOADING DENSITY OF 1.65 g/cm <sup>3</sup> . . . . .	35

Page intentionally blank

Page intentionally blank

Page intentionally blank

# SYMBOLS

- $c$  = sound speed =  $\left(\frac{\partial p}{\partial \rho}\right)_s^{1/2}$   
 $D$  = detonation velocity  
 $E$  = internal energy of explosion products at  $(T,p)$   
 $E_0$  = internal energy of explosion products at  $300^\circ \text{ K}$  and  $1 \text{ atm}$   
 $E-E_0$  = internal energy of explosion products  
 $p$  = pressure  
 $\Delta Q$  = chemical energy  
 $r$  = distance from point of initiation  
 $s$  = entropy  
 $T$  = temperature  
 $t$  = time  
 $u$  = mass velocity  
 $v$  = specific volume ( $= 1/\rho$ )  
 $\gamma$  =  $-\left(\frac{\partial \ln p}{\partial \ln v}\right)_s$   
 $\lambda$  =  $r/t$   
 $\xi$  =  $u/\lambda$   
 $\rho$  = density  
 $\sigma$  =  $\int_{p_1}^p \frac{dp}{\rho c}$  ;  $p_1$  = detonation front value of  $p$   
 $\psi$  =  $u/c$



Page intentionally blank

Page intentionally blank

Page intentionally blank

## INTRODUCTION

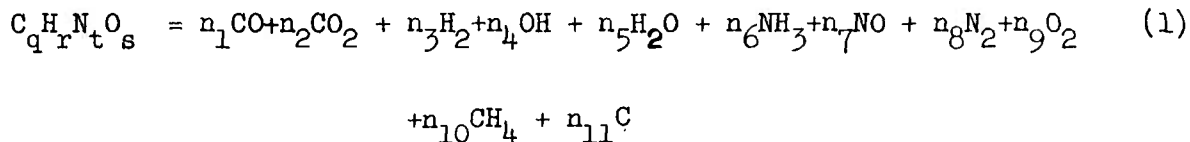
According to the hydrodynamic theory of detonation the properties of the detonation front in an explosive are determined by the conditions of:

- (1) conservation of mass, momentum and energy
- (2) the Chapman-Jouguet hypothesis
- (3) the equation of state for the explosion products
- (4) the distribution of the chemical elements in the explosive among possible molecular species of the product composition.

Because of inadequate knowledge of the behavior of gases and solids at the high temperatures and pressures encountered in detonation processes the choice of a suitable equation of state presents a formidable problem. Several equations of state have been proposed by other investigators (for a brief summary, see Reference 1). The equation of state used here is the equation used extensively by Brinkley and Wilson (Ref. 2). With their equation of state, Brinkley and Wilson obtained reasonable agreement with observed detonation velocities for a variety of explosives.

Pentolite has been used extensively in the experimental study of blast parameters (see Ref. 3 for compilation of blast data) and, therefore, it is of interest to determine the detonation characteristics of this explosive.

The explosive 50-50 pentolite is a mixture of equal weights of the explosives PETN and TNT. If a "molecular weight" of 250 grams for pentolite is assumed its chemical formula may be written symbolically as  $C_{5.825} H_{5.81} N_{3.23} O_{8.04}$ . Additionally, it is assumed that the detonation process gives rise to the reaction



where for pentolite

$$\begin{aligned}
 q &= 5.825 = n_1 + n_2 + n_{10} + n_{11} \\
 r &= 5.910 = 2n_3 + n_4 + 2n_5 + 3n_6 + 4n_{10} \\
 t &= 3.230 = n_6 + n_7 + 2n_8 \\
 s &= 8.040 = n_1 + 2n_2 + n_4 + n_5 + n_7 + 2n_9
 \end{aligned}
 \tag{2}$$

The distribution of the atoms among these molecular species (products) is determined by assuming several chemical reactions and the conditions of thermodynamic equilibrium. With these assumptions and the above atom-balance equations a solution, consistent with the conditions imposed by the equations describing the detonation process, is obtained.

The values of the parameters at the detonation front are used as initial conditions for the determination of the isentropic expansion of the explosion products. The data, thus obtained, are sufficient for the determination of the initial pressure of the shock wave formed in the neighborhood of the detonating explosive. The results are sufficient to determine a progressive wave solution of the distribution of pressure and velocity behind the detonation front.

#### CONDITIONS AT THE DETONATION FRONT

Across the detonation front the usual conditions of the conservation of mass, momentum and energy hold. These conditions for  $u_0 = 0$ , are: (see Ref. 4)

$$\begin{aligned}
 (a) \quad \rho_0 D &= \rho_1 (D - u_1) \\
 (b) \quad p_0 + \rho_0 D^2 &= p_1 + \rho_1 (D - u_1)^2 \\
 (c) \quad E_1 - E_0 &= \Delta Q + 1/2 \left( \frac{1}{\rho_0} - \frac{1}{\rho_1} \right) (p_1 + p_0)
 \end{aligned}
 \tag{3}$$

where  $\Delta Q$  represents the difference between the heats of formation of the product species and the explosive, i.e.,  $\Delta Q = \sum_i^n H_i - H_{f, \text{explosive}}$ . The  $H_i$  are given in Table 1 and  $H_{f, \text{explosive}}$  is taken to be 57.688kcal/250 g pentolite. The explosive pentolite in its condensed state, is assumed to be at rest, of density 1.65 g/cm<sup>3</sup> and in air at one atmosphere pressure and 300°K. In these Laboratories the normal loading density of pentolite is 1.65 g/cm<sup>3</sup>.

Equations (3) are to be supplemented by the Chapman-Jouguet hypothesis which states that the detonation velocity, D, is the minimum wave velocity compatible with the conditions imposed by the conservation equations and the given initial state of the explosive. Equations (3), along with the equation of state, determine a one-parameter family of solutions and the solution for which

$$\left(\frac{dp}{dv}\right)_{\text{Hugoniot}} = \frac{p-p_0}{v-v_0}; \quad \text{where } v = 1/\rho \quad (4)$$

determines the conditions at the wave front (Reference 4). Equation (4) is equivalent to the Chapman-Jouguet hypothesis. Furthermore, it follows that  $D = u+c$  for a Chapman-Jouguet detonation (Reference 4).

#### EQUATION OF STATE

The equation of state used here is the Brinkley-Wilson equation (Reference 2) viz.,

$$p(v-\eta v_s) = \frac{n_g RT(1+xe^{\beta x})}{M} = \frac{n_g RT F(x)}{M} \quad (5)$$

$$\text{where} \quad x = \frac{\sum_i^n k_i}{M(v-\eta v_s)T^{\alpha}} \quad (6)$$

$\alpha = 1/4$ ,  $\beta = 3/10$ ,  $n_g$  is the number of moles of gaseous products,  $\eta$  is the weight fraction of the solids products,  $v_s$  is the specific volume of the solids and the  $k_i$  are covolume constants and are presented in Table 2.

Assuming that  $M = 250$  grams and that the only solid product in the explosion products is graphite of density  $2.25 \text{ g/cm}^3$  and that the volume change of the graphite is negligible, the form of the equation of state becomes

$$p(V - 16/3 n_{11}) = n_g RTF(x); \quad V = Mv \quad (7)$$

From thermodynamic considerations and equation (7) the equation for the change in internal energy of  $M$  grams of explosion products is

$$E_1 - E_0 = \sum_{i=1}^{10} n_i \left[ E_i^0(T) - E_i^0(300^\circ\text{K}) \right] + n_{11} \int_{300}^T (C_p^0)_{\text{graphite}} dT + 1/4 n_g RT x e^{0.3x} \quad (8)$$

where  $E_i^0(T) - E_i^0(300^\circ\text{K})$  and  $\int_{300}^T C_p^0 dT$  are given in Table 3. The entropy of  $M$  grams of the explosion products is

$$S/R = \sum_{i=1}^{11} n_i \frac{S_i^0(T)}{R} - \sum_{i=1}^{10} n_i \ln \frac{n_i}{n_g} - n_g \left[ \ln \frac{82.054 n_g}{K} + \ln x - 1/4 x e^{0.3x} - \frac{10}{3} (1 - e^{0.3x}) + \frac{5}{4} \ln T \right] \quad (9)$$

where  $\frac{S_i^0}{R}(T)$  is given in Table 4 and  $K = \sum_{i=1}^{10} n_i K_i$ . From equations (8) and (9) the Helmholtz function  $A = E - TS$  becomes

$$A = \sum_i n_i A_i^0(T) + RT \sum_{i=1}^{10} n_i \ln n_i + n_g RT \left[ \ln x - \frac{10}{3} (1 - e^{0.3x}) - \ln(K/RT^{5/4}) \right] \quad (10)$$

# CONDITIONS FOR THERMODYNAMIC EQUILIBRIUM

The general conditions for thermodynamic equilibrium are:

$$(\Delta A)_{T,V} = 0 \quad (11)$$

and

$$\sum_i \nu_i \phi_i = 0 \quad (\text{constant } T, V) \quad (12)$$

where

$$\phi_i = \left( \frac{\partial A}{\partial n_i} \right)_{T,V} \quad (13)$$

and where the  $\nu_i$ 's are the stoichiometric coefficients of the reaction under consideration. Now, from (10) and (13)

$$\begin{aligned} \phi_i &= A_i^0(T) + RT \ln n_i + RT \\ &\quad - n_g RT k_i / K + RT \left[ \ln x \frac{10}{3} (1 - 3^{0.3x}) - \ln (K/RT^{5/4}) \right] \\ &\quad + n_g RT F(x) \frac{1}{x} \left( \frac{\partial x}{\partial n_i} \right) \end{aligned} \quad (14)$$

and at equilibrium

$$\begin{aligned} \sum_i \nu_i \phi_i = 0 &= \sum_i \nu_i (A_i^0(T) + RT) + RT \left\{ \sum_i \nu_i \ln n_i - n_g \frac{\sum_i \nu_i k_i}{K} \right. \\ &\quad \left. + \left[ \ln x - \frac{10}{3} (1 - e^{0.3x}) - \ln K/RT^{5/4} \right] \sum_i \nu_i + n_g F(x) \frac{1}{x} \sum_i \nu_i \frac{\partial x}{\partial n_i} \right\} \end{aligned} \quad (15)$$

Now  $\sum_i \nu_i [A_i^0(T) + RT] = -RT \ln K_{pj}^0$  where  $K_{pj}^0$  is the ideal equilibrium constant of the  $j$ th reaction and is dependent on the temperature. Thus, (15) can be rewritten as

$$\begin{aligned} \sum_i \nu_i \ln n_i &= \ln K_{pj}^0 - \left\{ \left[ \ln p/n_g F(x) + 10/3 (e^{0.3x} - 1) \right] \sum_i \nu_i \right\} \\ &\quad + n_g x e^{0.3x} \frac{\sum_i \nu_i k_i}{K} + \frac{p}{RT} \sum_i \nu_i v_{s_i} m_i \end{aligned} \quad (16)$$

If  $\xi_j$  is defined by the expression

$$-\ln \xi_j = \left[ \ln \frac{p}{n_g F(x)} + \frac{10}{3} (e^{0.3x} - 1) \right] \sum v_i + n_g x e^{0.3x} \frac{\sum v_i k_i}{K} + \frac{p}{RT} \sum v_i v_{s_i} m_i \quad (17)$$

then, from (16) and (17)

$$\prod_i (n_i)^{v_i} = K_{pj}^0 \xi_j = K_j \quad (18)$$

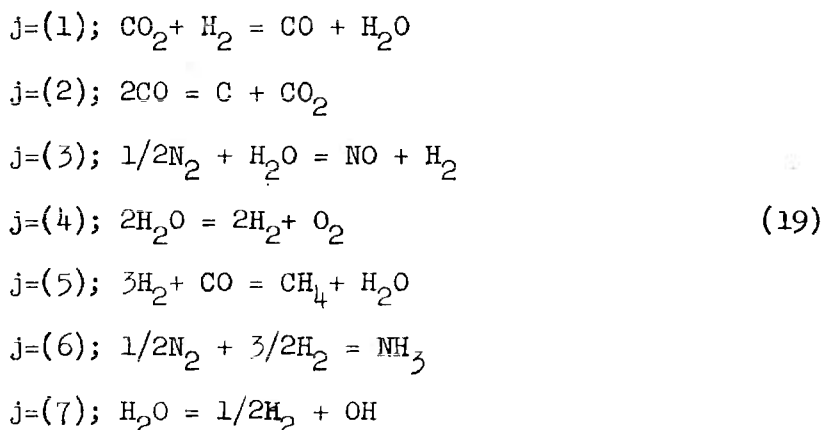
jth reaction

which is the desired condition on the number of moles,  $n_i$ , in the jth reaction. Values of  $K_{pj}^0$  were obtained from the equation (Ref. 5)

$$-\ln K_{pj}^0 = \frac{\Delta E_{pj}^0}{RT} - \sum_{i=1}^n \left( \left[ -\frac{F_i^0 - E_{oi}^0}{RT} \right]^{v_i} \right) \quad (\text{jth reaction})$$

$F_i^0 - E_{oi}^0$

The values of  $-\frac{F_i^0 - E_{oi}^0}{RT}$  and  $\Delta E_{pj}^0$  were obtained from references (10 and 11) and the calculated values of  $K_{pj}^0$  are given in Table 5. In the determination of the chemical composition of the explosion product mixture the following reactions are assumed



where the numerical values of  $j$  denotes the jth reaction. Hence, from equations (18) and the reactions (19) there follows

$$\begin{aligned}
K_1 &= n_1 n_5 / n_2 n_3 \\
K_2 &= n_2 / n_1^2 \\
K_3 &= n_7 n_3 / n_5 n_8^{1/2} \\
K_4 &= n_3 n_9 / n_5^2 \\
K_5 &= n_{10} n_5 / n_3^2 n_1 \\
K_6 &= n_6 / n_3^{3/2} n_8^{1/2} \\
K_7 &= n_4 n_3^{1/2} / n_5
\end{aligned} \tag{20}$$

and from (20) and the atom-balance equations (2) follows the system of equations for the determination of the  $n_i$ 's:

$$\begin{aligned}
n_1 &= \frac{-1 + \sqrt{1 + 4K_2 G}}{4K_2} \quad \text{where } G = 2s - r + 2n_3 + 3n_6 + 4n_{10} - n_4 - 2n_7 - 4n_9 \\
n_2 &= n_1^2 K_2, \\
n_3 &= n_1 n_5 / n_2 K_1, \\
n_4 &= n_5 K_7 / \sqrt{n_3}, \\
n_5 &= r - s + n_1 + 2n_2 + n_7 + 2n_9 - 2n_3 - 3n_6 - 4n_{10}, \\
n_6 &= n_3 \sqrt{n_8 n_3} K_6, \\
n_7 &= \frac{n_5 \sqrt{n_8}}{n_3} K_3, \\
n_8 &= 1/2(t - n_6 - n_7), \\
n_9 &= n_5^2 K_4 / n_3^2 \\
n_{10} &= n_3^3 n_1 K_5 / n_5 \\
n_{11} &= q - n_1 - n_2 - n_{10}
\end{aligned} \tag{21}$$



where  $n_1$  refers to the number of moles of CO,  $n_2$  the number of moles of CO<sub>2</sub>, etc. (See equation 2).

The conditions at the detonation front are determined by solving equations (3), (4), (6), (7), (8), and (21). To obtain the conditions at the wave front the Hugoniot curve in the neighborhood of the detonation point must be determined. The following iterative procedure was used to determine the Hugoniot curve. Starting with any value of  $T \geq 3000^\circ\text{K}$  and appropriate values of  $p^{(0)}$ ,  $v^{(0)}$ ,  $x^{(0)}$ , and  $n_i$ 's, consistent with the atom-balance equations, the equation

$$\frac{(\Delta Q)^{(0)} - \sum_{i=1}^{11} n_i^{(0)} e_i(T)}{n_g T} = 0.49680 x^{(0)} e^{0.3x^{(0)}} - \frac{0.99363(v_0 - v^{(1)})}{v^{(1)16/3} n_{11}^{(0)}} F(x^{(0)}) \quad (22)$$

obtained from equations (3), (7), and (8) is solved for  $v^{(1)} \text{ cm}^3/250 \text{ g pentolite}$ .

The symbol  $e_i(T)$  denotes  $E_i^0(T) - E_i^0(300^\circ\text{K})$  for  $i = 1, 2, \dots, 10$  and  $\int_{300}^T C_p dT$  for  $i = 11$ .  $p^{(1)}$  is then obtained from the equation of state

$$p^{(1)} = \frac{82.054 n_g^{(0)} T F(x^{(0)})}{v^{(1)16/3} n_{11}^{(0)}} \quad (7)$$

With these values of  $p^{(1)}$ ,  $v^{(1)}$  and  $T$ ,  $x^{(0)}$  and  $n_i^{(0)}$ 's improved values,  $n_i^{(1)}$ 's, of the  $n_i$ 's are obtained by solving equations (18) and (21) and  $x^{(1)}$  is obtained from the relation

$$x^{(1)} = \frac{K^{(1)}}{[v^{(1)16/3} n_{11}^{(0)}] T^{1/4}} \quad (6)$$

where  $K^{(1)} = \sum_{i=1}^{10} n_i^{(1)} k_i$ . By increasing superscripts by one in equation (11) and improved value  $v^{(2)}$  is obtained from equation (11) and improved values of the remaining quantities are obtained as above. The process is continued

until the convergence criteria  $|p^{(j)} - p^{(j-1)}| < 10^{-\alpha} p^{(j)}$ ;  $|v^{(j)} - v^{(j-1)}| < 10^{-\alpha}$  and  $|x^{(j)} - x^{(j-1)}| < 10^{-\alpha} x^{(j)}$  and  $|n_i^{(j)} - n_i^{(j-1)}| < 10^{-\beta} n_i^{(j)}$  are satisfied. For these calculations  $\alpha$  and  $\beta$  are chosen such that  $6 \leq \alpha \leq \beta \leq 9$ .

The converged values of  $p$ ,  $V$ ,  $x$ ,  $n_1$  and  $T$  determine a "point" on the Hugoniot curve. By assuming different values of  $T$  additional points on the Hugoniot can be determined by the above process. The detonation conditions are determined by locating the point,  $p$ ,  $V$  and  $T$  on the Hugoniot curve which satisfies the condition that  $(\frac{dp}{dV})_H = \frac{p-p_0}{V-V_0}$  where  $p_0 = 1$  atm,  $V_0 = 151.5 \text{ cm}^3/250 \text{ g pentolite}$  and where the differentiation refers to the Hugoniot curve. The computed detonation values are

$$\begin{aligned} p_1 &= 231250 \text{ atm} \\ V_1 &= 116.19 \text{ cm}^3/250 \text{ g pentolite} \\ T_1 &= 3367.7^\circ\text{K} \\ D &= 7807 \text{ m/sec} \end{aligned}$$

Gehring and Dewey (Ref. 7), report experimentally determined values of

$$\begin{aligned} p_1 &= 237000 \text{ atm} \\ D &= 7620 \text{ m/sec} \end{aligned}$$

and  
for pentolite of density  $1.655 \text{ g/cm}^3$ .

#### ISENTROPIC EXPANSION OF THE EXPLOSION PRODUCTS

In general, the explosion products are a mixture of gases and solids and when such a mixture expands isentropically the chemical composition will change due to varying equilibrium conditions. In determining the isentropic expansion it is assumed that thermodynamic equilibrium exists throughout the initial phase of the expansion.

If the expansion is isentropic then the condition that

$$S_{m_1}(T_1) = S_{m_2}(T_2) \quad (23)$$

holds throughout the expansion. The subscripts  $m_1$  and  $m_2$  indicates that the chemical composition of the mixture at  $T_1$  may be different than that at  $T_2$ . The procedure followed in the calculation of the isentropic is to let  $T$  be the independent variable and to calculate the pressure, volume and equilibrium

composition at  $T$ . The starting conditions for the calculation of the isentrope are the detonation front values of  $T$ ,  $p$ , and  $V$ . The detonation front values are indexed by subscript one, i.e.,  $p_1$ ,  $V_1$ ,  $T_1$ ,  $x_1$ ,  $n_{i,1}$ ,  $i = 1, 2, \dots, 11$ . The entropy  $S_{m_1}(T_1)$  of the mixture of explosion products is calculated from equation (9) and Table 6. It is assumed that this value of the entropy remains constant throughout the expansion. If  $T_2$  is such that  $T_1 - 100 \leq T_2 \leq T_1$  the values of  $p$ ,  $V$  and the  $n_i$ 's at  $T_2$  can be determined as follows.

An approximate value of the equation of state variable,  $x$ , at  $T_2$ , is obtained from equation (23) by initially assuming that the chemical composition remains invariant. With this initial assumption  $x_2^{(o)}$  is obtained by solving the equation

$$\ln x_2^{(o)} + 10/3(1 - 0.075x_2^{(o)}) e^{0.3x_2^{(o)}} = \left(\frac{10}{3} - \frac{1}{4}x_1\right)e^{0.3x_1} + \ln x_1 + \frac{5}{4} \ln \frac{T_1}{T_2} - \frac{1}{n_g} \sum_{i=1}^{11} n_{i,1} \left[ \frac{S_i^0(T_1) - S_i^0(T_2)}{R} \right] \quad (24)$$

and then  $V_2^{(o)}$  is obtained from the definition of  $x$ , i.e.,

$$V_2^{(o)} = \frac{\sum_{i=1}^{11} n_i k_i}{x_2^{(o)} T_2^{1/4}} + \frac{16}{3} n_{11,1}$$

Substitution of  $x_2^{(o)}$ ,  $V_2^{(o)}$  and  $T_2$  into equation (7) gives  $p_2^{(o)}$ . With these approximate values of  $x$ ,  $p$  and  $V$  at  $T_2$  the values of  $K_j$  are obtained from equations (18) for each of the reactions (19) and then from equations (21) the corresponding  $n_i$ 's are obtained by iteration. From equation (9) and the definition of  $x$  (6) equation (15) is obtained.

$$x = -4.01324268 + \frac{10}{3} \ln G \quad (25)$$

$$\text{where } G = \frac{1}{n_g} \sum_{i=1}^{11} n_i \frac{S_i}{R}(T_2) - \frac{1}{n_g} \sum_{i=1}^{11} n_i \ln n_i + \ln \frac{V - \frac{16}{3} n_{11}}{T_2} + \frac{1}{328.216} \frac{p(V - \frac{16}{3} n_{11})}{n_g T_2} - 1.3240442338 - \frac{S/R(T_1)}{n_g}$$

The above calculated  $n_1$ 's,  $p_2^{(0)}$ , and  $V_2^{(0)}$  are used to obtain a second approximation to  $x_2$  from (25) and the  $V_2^{(1)}$ ,  $p_2^{(1)}$  and  $n_1^{(2)}$ 's are obtained as above. This process continues until convergence of the values of the parameters is obtained. The values calculated at  $T_2$  thus represent a "point" on the isentrope. The calculation then proceeds from  $T_2$  to  $T_3$  by the same process as indicated above. The expansion with varying chemical composition is continued until  $T = 1840^\circ\text{K}$  where it is arbitrarily assumed that for temperatures less than  $1840^\circ\text{K}$  the composition remains frozen. The results of the computation are presented in Tables 6 and 6a and Figure 1. Table 6 includes calculated values of

$$c = \left(\frac{\partial p}{\partial \rho}\right)_S^{1/2}; \quad \gamma = -\left(\frac{\partial \ln p}{\partial \ln V}\right)_S; \quad W = \int_{V_1}^V p \, dV; \quad \sigma = \int_{p_1}^p \frac{dp}{\rho c}; \quad \Delta Q; \text{ and}$$

$$E - E_0 \text{ (eq. 4)}$$

#### CALCULATION OF THE INITIAL SHOCK PRESSURE IN AIR

When an explosive is detonated the detonation wave travels through the explosive until it reaches the surface of the charge. Produced at the surface is a shock wave in air and a rarefaction wave in the explosion products. The shock wave moves outward into the air and the rarefaction wave travels backward through the explosion products. The explosion product - air boundary moves outward also but at a slower rate than the shock wave. When the wave is normal to the surface dynamical considerations require that pressure and mass velocity be equal across this boundary. The mass velocity in the explosion products at the boundary is given by (Ref. 4).

$$u = u_1 + \int_p^{p_1} \frac{dp}{\rho c} \quad (26)$$

where the subscript (1) refers to the detonation front. In air, the velocity and pressure are related by the Hugoniot conditions; i.e.,

$$u = u(p) \quad (27)$$

The integral in equation (26) is tabulated in Table 6 and the condition (27) is tabulated by Shear and Day (Ref. 7). Using these data, equations (26) and (27) were solved, graphically, and an initial shock pressure of 670 atm was obtained. This value depends on the temperature where the composition is frozen since when the composition was frozen at  $2390^{\circ}\text{K}$  the value of  $p$  was 663 atm. Sultanoff (Ref. 8) reports an experimental value of 818 atm. The accuracy of this measurement is uncertain since the method by which it was determined is essentially an extrapolation procedure and is dependent on the method of data reduction.

Holt (Ref. 12) has calculated the initial pressure of the shock wave formed in air at the surface of PETN. He reports a pressure value of 675 atm. Jones and Miller (Ref. 13) give the adiabatic expansion of the explosion of TNT at a loading density of  $1.5\text{g/cm}^3$ . The data reported by Jones and Miller are sufficient to determine the initial pressure of the shock formed in air at the surface of TNT. The present author made approximate calculation from this data and obtained a value of 515 atm.

#### PRESSURE AND VELOCITY DISTRIBUTION BEHIND PLANE AND SPHERICAL DETONATION FRONTS

The specification of the conditions at the detonation front and of the pressure-volume relation during the isentropic expansion of the explosion products provides the data necessary for the determination of the pressure and velocity distribution behind the front. The general problem was considered first by G. I. Taylor (Ref. 9) who applied the results of his analysis to obtain the pressure and velocity profile behind the detonation wave in TNT. Taylor assumed that the detonation velocity,  $D$ , is constant and that the time necessary to establish the detonation is negligible. With these assumptions all parameters behind the front are functions of  $\lambda = r/t$  where  $r$  is the radial distance from the point of initiation and  $t$  is the time given by  $R/D = R/(u_1 + c_1)$  where  $R$  is the distance of the detonation front from the point of initiation. The equations describing the flow behind a spherical front are

$$\frac{\partial \rho}{\partial t} + u \frac{\partial \rho}{\partial r} + \rho \frac{\partial u}{\partial r} = - \frac{2\rho u}{r} \quad (28)$$

$$\frac{\partial u}{\partial t} + u \frac{\partial u}{\partial r} = - \frac{c^2}{\rho} \frac{\partial \rho}{\partial r}$$

and the condition that  $\rho$ ,  $u$ , and  $p$  depend on  $\lambda = r/t$  is expressed by

$$L(u; p; \rho) = 0 \text{ where } L = \frac{\partial}{\partial t} + \lambda \frac{\partial}{\partial r} \quad (29)$$

Following Taylor and introducing the variables

$$\xi = u/\lambda, \quad \psi = u/c \quad \text{and } Z = \ln \lambda \quad (30)$$

equations (27) and (28) become

$$\frac{d\psi}{dZ} = \frac{\psi \xi}{(1-\xi)^2 \psi^2 - \xi^2} \{ 2\xi - (1-\xi) \psi^2 f \} \quad (31)$$

$$\frac{d\xi}{dZ} = \xi \frac{3\xi^2 - (1-\xi)^2 \psi^2}{(1-\xi)^2 \psi^2 - \xi^2}$$

where 
$$f = \frac{\rho}{c^2} \frac{dc^2}{d\rho}$$

Since  $R = D t$  and  $\lambda = r/t$ ; there follows the relation

$$\lambda/D = r/R \quad (32)$$

Noting that  $Z$  appears only as a differential,  $dZ$ , in (20) its value may be taken as

$$Z = \ln r/R \quad (33)$$

From (32) and (33) and the definitions of  $\xi$  and  $\psi$  there follows the relations

$$u/D = \xi \ r/R \quad (34)$$

$$\phi = c/D = \frac{\xi}{\psi} r/R$$

Since  $c$  has been determined (Table 6)  $\phi$  may be taken as the independent variable by using the transformation defined by

$$\frac{d\phi}{\phi} = - \frac{d\psi}{\psi} + \frac{d\xi}{\xi} + dZ \quad (35)$$

Thus, there follows from (31)

$$\begin{aligned} \frac{d\psi}{d\phi} &= \frac{2\xi - (1-\xi)\psi^2 f}{\phi(1-\xi)\psi f} \\ \frac{d\xi}{d\phi} &= \frac{3\xi^2 - (1-\xi)^2 \psi^2}{\phi(1-\xi)\psi^2 f} \end{aligned} \quad (36)$$

and where  $Z$  can be determined from (33) and (34) or from

$$\frac{dZ}{d\phi} = \frac{(1-\xi)^2 \psi^2 - \xi^2}{\phi(1-\xi)\xi \psi^2 f} \quad (37)$$

The calculation of the above equations proceeds inward from the front where the initial values of  $Z$ ,  $\xi$ ,  $\psi$  and  $\phi$  are:

$$\begin{aligned} \xi_1 &= \frac{u_1}{x_1} = \frac{u_1}{u_1 + c_1} = 1 - \frac{\rho_0}{\rho_1} = 0.23315 \\ \psi_1 &= \frac{u_1}{c_1} = \frac{\rho_1}{\rho_0} - 1 = 0.30403 \end{aligned} \quad (38)$$

$$\phi_1 = c_1/D = \rho_0/\rho_1 = 0.76685$$

$$Z = 0, \ r/R = 1$$

The solution of (36) is tabulated in Table 7 and  $p$  and  $u/D$  are plotted versus  $r/R$  in Figure 2 and 3. The particle velocity,  $u$ , becomes zero at  $r/R = 0.43$  and the mass of the explosion products contained between  $r/R = 0.43$  and  $r/R = 1$  is approximately 233 grams which is about 93 % of the total mass of explosion products.

For comparison, the particle velocity and pressure distribution vs.  $r/R$  behind a plane detonation wave are shown in Figure 2 and 3. The results shown for the plane detonation wave are those which correspond to the physical model of a detonation wave traveling in a rigid walled tube closed at the end where initiation takes place. If the detonation wave is planar then behind the front constant values of  $u$ ,  $\rho$  and  $c$  travel with the speed  $u + c$  and  $u$  is given by

$$u_1 + \int_{p_1}^p \frac{dp}{\rho c} = u$$

where  $u_1$  and  $p_1$  are, respectively, the detonation front values of particle velocity and pressure. The integral has been tabulated in Table 6 and thus  $u$  can be determined for various values of  $p$  and the corresponding values of  $\rho$  and  $c$  are known from the adiabatic expansion (Table 6). Thus, pressure and particle velocity are determined as functions of  $r/R = (u+c)/D$  where  $r$  and  $R$  are defined as before.

For the spherical wave front calculations the chemical energy released when  $u = 0$  is 1.162 kcal/g and the temperature is, approximately, 2390°K. The detonation front value of  $\Delta Q$  is 1.109 kcal/g and when the composition of the explosion products is frozen  $\Delta Q$  is 1.186 kcal/g. Since  $p$  and  $u$  are known (from 36) the corresponding values of  $E - E_0$  can be determined and the total energy,  $E_{tot}$ , carried by the wave motion can be calculated. Now  $E_{total} = E_{kinetic} + E_{internal}$  where

$$E_{int} = 4\pi R^3 \int_0^1 (E - E_0) \rho \left(\frac{r}{R}\right)^2 d\left(\frac{r}{R}\right) / 4\pi R^3 \int_0^1 \rho \left(\frac{r}{R}\right)^2 d\left(\frac{r}{R}\right)$$



$$E_{kin} = 4\pi R^3 \int_0^1 \frac{1}{2} \rho u^2 (r/R)^2 d(r/R) / 4\pi R^3 \int_0^1 \rho (r/R)^2 d(r/R)$$

From the solution of equation (36) and the properties along the adiabetic the calculated values of  $E_{int}$  and  $E_{kin}$  are 1.063 kcal/g and 0.084 kcal/g and  $E_{total} = 1.152$  kcal/g and the distribution of energy between internal and kinetic is approximately 93 % internal and 7% kinetic.

#### CONCLUSION

The calculated values of the detonation pressure and velocity are 231350 atm and 7807 m/sec respectively. These values agree to within 2-1/2% with the corresponding experimental values reported by Gehring and Dewey (Ref. 6). The calculated initial pressure of the shock wave formed in air is about 18% lower than Sultanoff's experimental determined value of 818 atm.

The chemical energy released at the detonation front is 1.109 kcal/g and when the composition is frozen the chemical energy released is 1.186 kcal/g. The total energy,  $E_{total}$ , carried by the wave motion is 1.152 kcal/g and its distribution between internal and kinetic energy is approximately 93% internal and 7% kinetic.

#### ACKNOWLEDGEMENTS

The author gratefully acknowledges the invaluable assistance received from P. R. Schlegel, B. T. Addison, H. Wisniewski and R. Abernethy who were responsible for coding and programming this problem on the EDVAC and ORDVAC computers.

*Ralph E. Shear*

RALPH E. SHEAR

# REFERENCES

1. Morris, G. and Thomas, H. The Hydrodynamic Theory of Detonation, I. Research I, 1947, p. 132.
2. Brinkley, S. R., Jr. and Wilson, E. B., Jr. Revised Method of Predicting The Detonation Velocities in Solid Explosives. OSRD 905, Division B, NDRC, OSRD, 1942.
3. Goodman, H. Compiled Free-Air Blast Data on Bare Spherical Pentolite. BRL Report No. 1092, Ballistic Research Laboratories, APG, Md., 1960.
4. Courant, R. and Friedrich, K. O. Supersonic Flow and Shock Waves. Interscience, 1948.
5. Herzberg, G. Infrared and Raman Spectra. Van Nostrand, 1945.
6. Gehring, J. W., Jr. and Dewey, J. An Experimental Determination of Detonation Pressure in Two Solid High Explosives. BRL Report No. 935, Ballistic Research Laboratories, APG, Md., 1955.
7. Shear, R. E. and Day, B. D. Tables of Thermodynamic and Shock Front Parameters for Air. BRL Memorandum Report No. 1206, Ballistic Research Laboratories, APG, Md., 1959.
8. Sultanoff, M. and McVey, G. Shock Pressure at and Close to the Surface of Spherical Pentolite Charges Inferred From Optical Measurement. BRL Report No. 917, Ballistic Research Laboratories, APG, Md., 1957.
9. Taylor, G. I. The Dynamics of the Combustion Products Behind Plane and Spherical Detonation Fronts in Explosives. Proc. Roy. Soc. (London) A-200, 1950, p. 235.
10. Hilsenrath, J. et al. Tables of Thermal Properties of Gases. National Bureau of Standards Circular 564, 1955.
11. Sarner, S. and Warlick, D. Thermodynamic Properties of Combustion Products. General Electric Company Rpt R59FPD796, Volume 3, General Electric Company, Cincinnati, Ohio, 1960.
12. Holt, M. The Initial Behavior of a Spherical Explosion, II; Application to PETN Charges in Air and Water. ARDE Symposium on Blast and Shock Waves, Fort Halstead, July 1955.
13. Jones, H. and Miller, A. R. The Detonation of Solid Explosives. Proc. Roy. Soc. (London) A-194, 1948, p. 480.

TABLE 1

Heats of Formation,  $H_i$  (cal/mole)

Chemical Specie	Index, i	$H_i$	Reference
CO	1	26413	9
CO <sub>2</sub>	2	94052	9
H <sub>2</sub>	3	0	9
O	4	-9358.9	10
H <sub>2</sub> O	5	57802	9
NH <sub>3</sub>	6	13469	10
NO	7	-21600	9
N <sub>2</sub>	8	0	9
O <sub>2</sub>	9	0	9
CH <sub>4</sub>	10	17904	10

TABLE 2

Covolume Constants (Ref. 2)

Species	Index, i	$k_i \text{ cm}^3 \text{ } ^\circ\text{K}^{-1/4} / \text{Mole}$
CO	1	386
CO <sub>2</sub>	2	687
H <sub>2</sub>	3	153
OH	4	108
H <sub>2</sub> O	5	108
NH <sub>3</sub>	6	164
NO	7	233
N <sub>2</sub>	8	353
O <sub>2</sub>	9	333
CH <sub>4</sub>	10	400

TABLE 3

Ideal Internal Energies Relative to 300°K (cal/mole)

Species	$e_i(T)$										
	CO	CO <sub>2</sub>	H <sub>2</sub>	OH	H <sub>2</sub> O	NH <sub>3</sub>	NO	N <sub>2</sub>	O <sub>2</sub>	CH <sub>4</sub>	C <sup>*</sup>
T°K	$e_1$	$e_2$	$e_3$	$e_4$	$e_5$	$e_6$	$e_7$	$e_8$	$e_9$	$e_{10}$	$e_{11}$
300	0	0	0	0	0	0	0	0	0	0	0
400	499.67	741.72	495.82	511.32	611.11	691.37	514.70	498.54	511.46	709.25	245.82
500	1007.1	1571.5	995.60	1018.3	1242.0	1455.3	840.01	1002.4	1043.9	1548.7	564.45
600	1528.0	2472.6	1497.0	1525.6	1897.7	2314.9	1577.5	1516.7	1600.4	2529.6	941.67
700	2065.5	3432.4	2000.4	2031.6	2580.3	3217.8	2134.1	2045.2	2179.6	3648.2	1366.2
800	2620.7	4441.3	2507.2	2545.5	3291.5	4193.7	2708.6	2589.6	2778.5	4896.1	1826.1
900	3192.8	5491.2	3019.6	3064.9	4032.3	5239.2	3300.4	3150.1	3393.8	6257.5	2311.8
1000	3780.0	6575.2	3539.0	3596.7	4803.4	6351.9	3907.3	3725.7	4022.7	7727.1	2818.2
1100	4380.3	7687.8	4066.6	4136.1	5604.8	7515.4	4438.3	4315.1	4662.9	9290.4	3340.9
1200	4993.1	8824.9	4603.4	4685.4	6435.9	8752.5	5159.3	4916.8	5312.6	10938	3877.2
1300	5616.2	9982.7	5150.5	5249.3	7295.6	10072	5797.8	5529.3	5970.6	12660	4424.3
1400	6248.0	11157	5707.9	5820.9	8182.5	11435	6445.1	6151.3	6635.8	14199	4980.5
1500	6887.4	12347	6276.2	6404.7	9094.9	12842	7099.8	6781.6	7307.8	16291	5544.1
1600	7533.4	13550	6854.8	7000.1	10031	14273	7761.0	7419.2	7986.0	18188	6114.2
1700	8185.2	14764	7443.2	7600.7	10989	15731	8425.6	8063.2	8670.2	20124	6689.3
1800	8842.6	15988	8040.8	8212.3	11968	17192	9091.7	8712.8	9360.2	22102	7267.9
1900	9504.2	17220	8648.2	8835.7	12965	18683	9769.4	9366.8	10056	24117	7849.4
2000	10170	18460	9264.8	9461.1	13979	20187	10445	10026	10757	26159	8433.5
2100	10840	19707	9889.5	10100	15010	21729	10707	10689	11464	28231	9020.8
2200	11512	20960	10522	10742	16054	23248	11805	11356	12177	30326	9611.2
2300	12188	22218	11163	11389	17113	24798	12491	12026	12895	32445	10204
2400	12866	23482	11810	12044	18184	26359	13179	12698	13618	34580	10798
2500	13546	24751	12465	12704	19266	27942	13870	13374	14347	36732	11394
2600	14229	26023	13126	13372	20358	29512	14558	14052	15081	38906	11994
2700	14914	27300	13793	14039	21461	31092	15255	14732	15820	41086	12595
2800	15601	28580	14466	14715	22572	32666	15952	15414	16564	43284	13198
2900	16289	29863	15145	15391	23692	34225	16649	16097	17314	45494	13802
3000	16979	31150	15830	16075	24820	35807	17345	16783	18068	47713	14408
3100	17670	32440	16520	16762	25958	37457	18046	17470	18826	49946	15016
3200	18363	33733	17215	17455	27097	39268	18750	18159	19590	52181	15626
3300	19058	35028	17916	18155	28278	40954	19447	18849	20357	54431	16237
3400	19754	36327	18622	18850	29400	42622	20155	19541	21128	56685	16850
3500	20450	37627	19333	19556	30563	44314	20857	20234	21904	58944	17464
3600	21148	38931	20048	20260	31726	46166	21568	20928	22684	61210	18080
3700	21848	40236	20768	20969	32899	47695	22272	21623	23466	63487	18696
3800	22547	41544	21494	21685	34072	49407	22985	22320	24252	65764	19314
3900	23248	42854	22223	22401	35254	51113	23693	23017	25043	68052	19932
4000	23951	44166	22956	23126	36436	52834	24408	23716	25836	70340	20552
4100	24654	45480	23694	23840	37624	54559	25114	24415	26632	72631	21172
4200	25358	46796	24436	24576	38816	56276	25831	25115	27430	74931	21793
4300	26063	48114	25182	25308	40012	58010	26543	25817	28232	77236	22414
4400	26769	49434	25933	26028	41212	59699	27260	26519	29036	79530	23036
4500	27476	50756	26687	26771	42414	61419	27975	27219	29842	81843	23658
4600	28184	52080	27445	27509	43620	63190	28698	27926	30650	84159	24281
4700	28892	53405	28208	28252	44828	64874	29413	28630	31462	86477	24905
4800	29601	54733	28975	28991	46041	66636	30139	29336	32274	88785	25529
4900	30311	56062	29746	29744	47255	68355	30849	30042	33088	91110	26154
5000	31022	57393	30520	30491	48473	70095	31572	30749	33905	93454	26779

$$* \quad e_{11} = \int_{300^{\circ}\text{K}}^T C_P^{\circ} dT$$

TABLE 3a

Ideal Internal Energy,  $E_{300}^{\circ} - E_0^{\circ}$  cal/mole, Relative to  $0^{\circ}\text{K}$

		Ref
CO	1489.2	10
CO <sub>2</sub>	1658.6	10
H <sub>2</sub>	1440.3	10
OH	1523.8	11
H <sub>2</sub> O	1785.4	10
NH <sub>3</sub>	1823.8	11
NO	1610.9	11
N <sub>2</sub>	1488.9	10
O <sub>2</sub>	1491.5	10
CH <sub>4</sub>	1815.4	11

TABLE 4  
Entropy (Ideal)  $S_i^0(T)/R$

Species	CO	CO <sub>2</sub>	H <sub>2</sub>	OH	H <sub>2</sub> O	NH <sub>3</sub>	NO	N <sub>2</sub>	O <sub>2</sub>	CH <sub>4</sub>	C
T°K	$\frac{S_1(T)}{R}$	$\frac{S_2(T)}{R}$	$\frac{S_3(T)}{R}$	$\frac{S_4(T)}{R}$	$\frac{S_5(T)}{R}$	$\frac{S_6(T)}{R}$	$\frac{S_7(T)}{R}$	$\frac{S_8(T)}{R}$	$\frac{S_9(T)}{R}$	$\frac{S_{10}(T)}{R}$	$\frac{S_{11}(T)}{R}$
300	23.782	25.727	15.726	22.106	22.722	23.201	25.353	23.050	24.686	22.418	0.697
400	24.792	27.085	16.732	23.134	23.894	24.484	26.385	24.060	25.714	23.728	1.053
500	25.585	28.239	17.516	23.927	24.825	25.561	27.197	24.849	26.534	24.891	1.409
600	26.245	29.247	18.158	24.575	25.069	26.527	27.873	25.502	27.227	25.971	1.753
700	26.816	30.145	18.703	25.122	26.292	27.374	28.459	26.066	27.830	26.992	2.082
800	27.323	30.956	19.177	25.601	26.903	28.159	28.979	26.566	28.366	27.962	2.392
900	27.779	31.696	19.598	26.027	27.460	28.897	29.447	27.016	28.849	28.887	2.679
1000	28.196	32.376	19.978	26.414	27.974	29.585	29.875	27.426	29.287	29.771	2.948
1100	28.571	33.005	20.327	26.768	28.454	30.236	30.227	27.804	29.690	30.616	3.197
1200	28.934	33.589	20.649	27.095	28.905	30.867	30.632	28.154	30.061	31.424	3.433
1300	29.265	34.136	20.949	27.403	29.331	31.475	30.969	28.481	30.406	32.198	3.654
1400	29.575	34.649	21.232	27.690	29.736	32.053	31.284	28.787	30.728	32.938	3.861
1500	29.866	35.131	21.498	27.962	30.121	32.605	31.580	29.075	31.031	33.647	4.055
1600	30.140	35.585	21.750	28.220	30.490	33.130	31.860	29.347	31.316	34.327	4.242
1700	30.400	36.016	21.990	28.463	30.843	33.631	32.124	29.604	31.585	34.979	4.418
1800	30.646	36.425	22.219	28.696	31.181	34.103	32.372	29.848	31.840	35.605	4.584
1900	30.880	36.815	22.438	28.920	31.507	34.565	32.611	30.080	32.084	36.207	4.746
2000	31.103	37.186	22.649	29.133	31.820	34.999	32.836	30.301	32.316	36.785	4.896
2100	31.316	37.541	22.851	29.339	32.122	35.427	33.052	30.513	32.538	37.343	5.037
2200	31.520	37.881	23.046	29.535	32.413	35.830	33.258	30.715	32.752	37.880	5.173
2300	31.716	38.207	23.233	29.725	32.694	36.222	33.456	30.910	32.957	38.398	5.304
2400	31.904	38.520	23.415	29.907	32.966	36.603	33.646	31.096	33.154	38.898	5.435
2500	32.084	38.822	23.590	30.084	33.229	36.962	33.828	31.276	33.345	39.381	5.560
2600	32.258	39.112	23.760	30.254	33.484	37.302	34.003	31.449	33.529	39.849	5.661
2700	32.426	39.392	23.924	30.419	33.731	37.634	34.174	31.616	33.707	40.301	5.777
2800	32.588	39.663	24.084	30.579	33.971	37.954	34.337	31.777	33.880	40.740	5.887
2900	32.744	39.925	24.239	30.734	34.204	38.258	34.496	31.933	34.047	41.165	5.994
3000	32.896	40.178	24.389	30.884	34.430	38.561	34.648	32.084	34.210	41.577	6.104
3100	33.043	40.423	24.536	31.031	34.650	38.857	34.797	32.230	34.368	41.979	6.200
3200	33.185	40.662	24.679	31.173	34.864	39.184	34.941	32.372	34.521	42.367	6.295
3300	33.324	40.894	24.818	31.312	35.072	39.477	35.079	32.509	34.671	42.747	6.391
3400	33.458	41.118	24.954	31.446	35.276	39.753	35.215	32.643	34.817	43.115	6.476
3500	33.589	41.337	25.087	31.578	35.474	40.030	35.347	32.773	34.959	43.473	6.577
3600	33.716	41.550	25.216	31.706	35.668	40.301	35.476	32.900	35.097	43.823	6.657
3700	33.839	41.757	25.343	31.831	35.856	40.554	35.600	33.023	35.233	44.164	6.748
3800	33.960	41.959	25.467	31.954	36.041	40.814	35.722	33.143	35.365	44.497	6.833
3900	34.078	42.156	25.589	32.074	36.221	41.062	35.841	33.260	35.494	44.821	6.914
4000	34.192	42.349	25.707	32.191	36.397	41.304	35.957	33.374	35.620	45.138	6.995
4100	34.305	42.537	25.824	32.305	36.5696	41.544	36.070	33.4861	35.7441	45.448	7.065
4200	34.414	42.721	25.937	32.418	36.7382	41.771	36.181	33.5951	35.8650	45.751	7.146
4300	34.521	42.900	26.049	32.528	36.9034	42.003	36.288	33.7017	35.9835	46.047	7.226
4400	34.626	43.076	26.159	32.635	37.0651	42.219	36.395	33.8059	36.0995	46.336	7.302
4500	34.728	43.248	26.267	32.741	37.2236	42.436	36.498	33.9079	36.2132	46.619	7.377
4600	34.828	43.417	26.373	32.844	37.3789	42.652	36.600	34.0077	36.3246	46.898	7.447
4700	34.927	43.582	26.477	32.947	37.5313	42.853	36.699	34.1055	36.4338	47.170	7.523
4800	35.023	43.743	26.579	33.046	37.6807	43.060	36.797	34.2013	36.5410	47.435	7.598
4900	35.117	43.902	26.680	33.145	37.8274	43.261	36.891	34.2952	36.6461	47.697	7.668
5000	35.209	44.057	26.779	33.241	37.9713	43.453	36.984	34.3873	36.7493	47.954	7.739

TABLE 5  
Equilibrium Constants\*

T°K	K <sub>p1</sub>	K <sub>p2</sub>	K <sub>p3</sub>	K <sub>p4</sub>	K <sub>p5</sub>	K <sub>p6</sub>	K <sub>p7</sub>
1000	0.6946	5.8009 (-1)	7.4287 (-15)	7.5515 (-21)	3.9207 (-2)	5.9808 (-4)	5.0979 (-12)
1100	1.0096	9.0169 (-2)	3.0198 (-13)	1.7213 (-18)	3.2934 (-3)	3.2391 (-4)	1.1702 (-10)
1200	1.3674	1.9305 (-2)	6.6515 (-12)	1.6030 (-16)	4.1665 (-4)	1.9465 (-4)	1.5962 (-9)
1300	1.7548	5.2861 (-3)	9.1242 (-11)	7.4785 (-15)	7.2288 (-5)	1.2582 (-4)	1.4622 (-8)
1400	2.1567	1.7544 (-3)	8.6537 (-10)	2.0329 (-13)	1.6005 (-5)	8.6248 (-5)	9.7808 (-8)
1500	2.5719	6.7776 (-4)	6.0796 (-9)	3.5633 (-12)	4.3570 (-6)	6.2218 (-5)	5.0815 (-7)
1600	2.9875	2.9714 (-4)	3.3630 (-8)	4.3858 (-11)	1.3948 (-6)	4.6859 (-5)	2.1515 (-6)
1700	3.3943	1.4406 (-4)	1.5230 (-7)	4.0267 (-10)	5.1155 (-7)	3.6479 (-5)	7.6855 (-6)
1800	3.7928	7.6216 (-5)	5.8290 (-7)	2.8990 (-9)	2.0974 (-7)	2.9155 (-5)	2.3862 (-5)
1900	4.1740	4.3311 (-5)	1.9356 (-6)	1.6973 (-8)	9.4563 (-8)	2.4052 (-5)	6.5811 (-5)
2000	4.5405	2.6088 (-5)	5.7279 (-6)	8.3484 (-8)	4.6283 (-8)	2.0088 (-5)	1.6410 (-4)
2100	4.8871	1.6551 (-5)	1.5280 (-5)	3.5335 (-7)	2.4306 (-8)	1.7164 (-5)	3.7533 (-4)
2200	5.2166	1.0995 (-5)	3.7319 (-5)	1.3135 (-6)	1.3516 (-8)	1.4906 (-5)	7.9481 (-4)
2300	5.5292	7.5837 (-6)	8.5923 (-5)	4.3506 (-6)	7.9536 (-9)	1.3112 (-5)	1.5804 (-3)
2400	5.8166	5.4320 (-6)	1.7789 (-4)	1.3082 (-5)	4.8885 (-9)	1.1682 (-5)	2.9622 (-3)
2500	6.0956	3.9927 (-6)	3.5299 (-4)	3.5965 (-5)	3.1387 (-9)	1.0428 (-5)	5.2861 (-3)
2600	6.3514	2.9778 (-6)	6.6648 (-4)	9.1665 (-5)	2.0789 (-9)	9.3506 (-6)	9.0150 (-3)
2700	6.5951	2.3015 (-6)	1.1998 (-3)	2.1790 (-4)	1.4280 (-9)	8.4846 (-6)	1.4798 (-2)
2800	6.8240	1.8080 (-6)	2.0697 (-3)	4.8719 (-4)	1.0066 (-9)	7.7591 (-6)	2.3423 (-2)
2900	7.0198	1.4564 (-6)	3.4453 (-3)	1.0314 (-3)	7.2806 (-10)	7.1192 (-6)	3.5940 (-2)
3000	7.2219	1.1962 (-6)	5.5292 (-3)	2.0740 (-3)	5.3994 (-10)	6.6133 (-6)	5.3515 (-2)
3100	7.3965	9.8419 (-7)	8.6464 (-3)	4.0079 (-3)	4.0697 (-10)	6.1219 (-6)	7.7998 (-2)
3200	7.5732	8.2396 (-7)	1.3081 (-2)	7.3848 (-3)	3.1374 (-10)	5.7536 (-6)	0.11033
3300	7.7111	7.0315 (-7)	1.9349 (-2)	1.3206 (-2)	2.4540 (-10)	5.4503 (-6)	0.15360
3400	7.8711	6.0012 (-7)	2.7935 (-2)	2.2703 (-2)	1.9466 (-10)	5.1301 (-6)	0.20883
3500	7.9921	5.2732 (-7)	3.9598 (-2)	3.8041 (-2)	1.5674 (-10)	4.8792 (-6)	0.28018
3600	8.1299	4.5888 (-7)	5.4879 (-2)	6.1485 (-2)	1.2849 (-10)	4.6533 (-6)	0.36839
3700	8.2363	4.0680 (-7)	7.4852 (-2)	9.7638 (-2)	1.0574 (-10)	4.4245 (-6)	0.47891
3800	8.3456	3.6275 (-7)	0.10040	0.15063	8.8352 (-11)	4.2487 (-6)	0.61252
3900	8.4211	3.2420 (-7)	0.13306	0.22866	7.4121 (-11)	4.0706 (-6)	0.77578
4000	8.5259	2.9258 (-7)	0.17279	0.33739	6.3299 (-11)	3.9101 (-6)	0.96766
4100	8.6069	2.6410 (-7)	0.22271	0.49034	5.4264 (-11)	3.7728 (-6)	1.1955
4200	8.6781	2.4195 (-7)	0.28288	0.69984	4.7029 (-11)	3.6288 (-6)	1.4618
4300	8.7585	2.2218 (-7)	0.35520	0.98189	4.0984 (-11)	3.5282 (-6)	1.7707
4400	8.8059	2.0608 (-7)	0.44252	1.3595	3.5940 (-11)	3.4106 (-6)	2.1293
4500	8.8488	1.9185 (-7)	0.54616	1.8585	3.1580 (-11)	3.3070 (-6)	2.5377
4600	8.8966	1.7866 (-7)	0.66617	2.5008	2.8074 (-11)	3.2100 (-6)	2.9991
4700	8.9420	1.6707 (-7)	0.80702	3.3308	2.4994 (-11)	3.1142 (-6)	3.5264
4800	8.9864	1.5714 (-7)	0.96849	4.3674	2.2481 (-11)	3.0376 (-6)	4.1103
4900	9.0122	1.4834 (-7)	1.1565	5.6867	2.0220 (-11)	2.9683 (-6)	4.7677
5000	9.0397	1.4079 (-7)	1.3670	7.3179	1.8314 (-11)	2.8842 (-6)	5.4935

\* See (19) of text.



TABLE 6

Thermodynamic Properties of the Explosion Products During Isentropic  
Expansion of the Wave Front in Pentolite at a Loading Density of 1.65 g/cm<sup>3</sup>

T °K	P <sub>atm</sub>	x	γ	ρ, g/cm <sup>3</sup>	c <sub>m</sub> /sec	-σ, m/sec	W $\frac{\text{Kcal}}{\text{g}}$	E - E <sub>0</sub> $\frac{\text{Kcal}}{\text{g}}$	ΔQ $\frac{\text{Kcal}}{\text{g}}$
3367.7	231347	3.3663	3.29	2.1516	5937	0	0	1.505	1.109
3300	211480	3.2950	3.34	2.0942	5843	160	0.068	1.448	1.120
3200	185228	3.1399	3.36	2.0129	5593	387	0.161	1.365	1.131
3100	161740	3.0834	3.34	1.9331	5325	607	0.246	1.287	1.138
3000	140602	2.9746	3.31	1.8535	5044	826	0.327	1.211	1.144
2900	121752	2.8643	3.26	1.7740	4761	1040	0.404	1.138	1.147
2800	104783	2.7513	3.20	1.6935	4482	1255	0.478	1.067	1.150
2700	89400	2.6336	3.14	1.6108	4201	1472	0.549	0.999	1.153
2600	75673	2.5125	3.07	1.5266	3926	1690	0.617	0.934	1.156
2500	63369	2.3865	3.00	1.4399	3655	1912	0.683	0.870	1.159
2400	52510	2.2562	2.90	1.3509	3382	2136	0.747	0.809	1.162
2300	42987	2.1214	2.82	1.2596	3120	2363	0.809	0.750	1.164
2200	34663	1.9811	2.72	1.1654	2863	2596	0.869	0.693	1.168
2100	27503	1.8363	2.62	1.0686	2612	2833	0.927	0.639	1.172
2000	21397	1.6862	2.50	0.9688	2367	3077	0.984	0.587	1.176
1900	16272	1.5312	2.38	0.8661	2131	3328	1.038	0.538	1.182
1800	12164	1.3742	2.36	0.7657	1969	3555	1.090	0.490	1.186
1700	9024.6	1.2202	2.25	0.6728	1751	3818	1.136	0.444	1.186
1600	6530.2	1.0655	2.15	0.5808	1563	4061	1.180	0.400	1.186
1500	4600.6	0.9125	2.05	0.4911	1390	4308	1.222	0.359	1.186
1400	3151.1	0.7642	1.92	0.4057	1230	4558	1.261	0.319	1.186
1300	2090.3	0.6229	1.81	0.3256	1086	4812	1.299	0.282	1.186
1200	1341.0	0.4924	1.71	0.2530	957	5070	1.334	0.246	1.186
1100	828.4	0.3751	1.61	0.1891	845	5331	1.368	0.212	1.186
1000	495.3	0.2760	1.52	0.1361	750	5593	1.400	0.180	1.186
900	283.1	0.1940	1.45	0.09337	667	5859	1.430	0.150	1.186
800	154.3	0.1301	1.39	0.06088	598	6129	1.459	0.121	1.186
700	79.35	0.0827	1.35	0.03747	539	6404	1.486	0.0942	1.186
600	37.95	0.0496	1.33	0.02161	486	6686	1.512	0.0685	1.186
500	16.46	0.0276	1.32	0.01150	438	6978	1.536	0.0442	1.186
400	6.205	0.0139	1.32	0.00549	389	7283	1.559	0.0214	1.186
300	1.873	0.0061	1.32	0.00233	339	7611	1.581	0.0003	1.186

TABLE 6a

Temperature, Volume and Number of Moles/250g Pentolite of Each Explosion Product  
During Isentropic Expansion of the Wave Front in Pentolite at a Loading Density of 1.65 g/cm<sup>3</sup>

T°K	$V_{250g \text{ Pentolite}}^{\text{cm}^3}$	CO	CO <sub>2</sub>	H <sub>2</sub>	OH	H <sub>2</sub> O	NH <sub>3</sub>	NO	N <sub>2</sub>	O <sub>2</sub>	CH <sub>4</sub>	C
3367.7	116.19	3.309	0.843	0.000	0.009	2.946	0.003	0.089	1.569	0.000	0.000	1.673
3300	119.38	3.285	0.872	-	0.007	2.946	0.003	0.058	1.584	-	-	1.668
3200	124.20	3.255	0.901	-	0.005	2.946	0.004	0.031	1.598	-	-	1.669
3100	129.32	3.218	0.928	-	0.004	2.946	0.005	0.016	1.604	-	-	1.678
3000	134.88	3.180	0.952	-	0.002	2.945	0.006	0.008	1.608	-	-	1.693
2900	140.92	3.154	0.969	0.001	0.002	2.943	0.007	0.004	1.610	-	-	1.702
2800	147.62	3.126	0.985	0.002	0.001	2.941	0.008	0.002	1.610	-	-	1.714
2700	155.20	3.094	1.003	0.003	0.001	2.938	0.010	-	1.610	-	-	1.727
2600	163.76	3.065	1.020	0.004	-	2.933	0.011	-	1.609	-	-	1.739
2500	173.63	3.024	1.044	0.007	-	2.927	0.013	-	1.608	-	-	1.756
2400	185.06	2.989	1.066	0.012	-	2.918	0.015	-	1.607	-	-	1.769
2300	198.47	2.951	1.091	0.019	-	2.906	0.018	-	1.606	-	0.001	1.781
2200	214.51	2.903	1.124	0.031	-	2.888	0.020	-	1.605	-	0.003	1.795
2100	233.95	2.844	1.167	0.048	-	2.862	0.022	-	1.604	-	0.006	1.808
2000	258.05	2.771	1.223	0.074	-	2.822	0.024	-	1.603	-	0.011	1.819
1900	288.64	2.681	1.297	0.109	-	2.765	0.025	-	1.602	-	0.021	1.826
1800	326.50	2.618	1.351	0.136	-	2.720	0.025	-	1.602	-	0.030	1.825

TABLE 7

Flow Properties Behind a Spherical Detonation Wave in Pentolite  
At a Loading Density of  $1.65 \text{ g/cm}^3$

$r/R$	$\xi$	$\psi$	$u/D$	$c/D$	$\rho \text{ g/cm}^3$	$p_{\text{atm}}$
1.00000	.233	.304	.233	.767	2.152	231350
.99985	.2280	.2990	.228	.762	2.136	225970
.9978	.2139	.2852	.213	.748	2.094	211480
.9933	.2010	.2724	.200	.733	2.053	197960
.9863	.1892	.2604	.187	.716	2.013	185230
.9767	.1782	.2488	.174	.700	1.973	173140
.9644	.1679	.2374	.162	.682	1.933	161740
.9492	.1581	.2259	.150	.664	1.893	150880
.9313	.1488	.2144	.138	.646	1.853	140600
.9104	.1397	.2026	.127	.628	1.814	130940
.8868	.1310	.1905	.116	.610	1.774	121750
.8609	.1225	.1781	.105	.592	1.734	113030
.8318	.1139	.1650	.095	.574	1.694	104780
.7992	.1049	.1507	.084	.556	1.652	96879
.7639	.0955	.1356	.073	.538	1.611	89400
.7255	.0856	.1193	.062	.520	1.569	82341
.6841	.0748	.1017	.051	.503	1.526	75673
.6392	.0626	.0824	.040	.486	1.483	69323
.5888	.0482	.0606	.028	.468	1.440	63370
.5297	.0300	.0353	.016	.450	1.396	57778
.4550	.0058	.0061	.003	.433	1.351	52510
.4300	.0000	.0000	.000	.430	1.342	51499

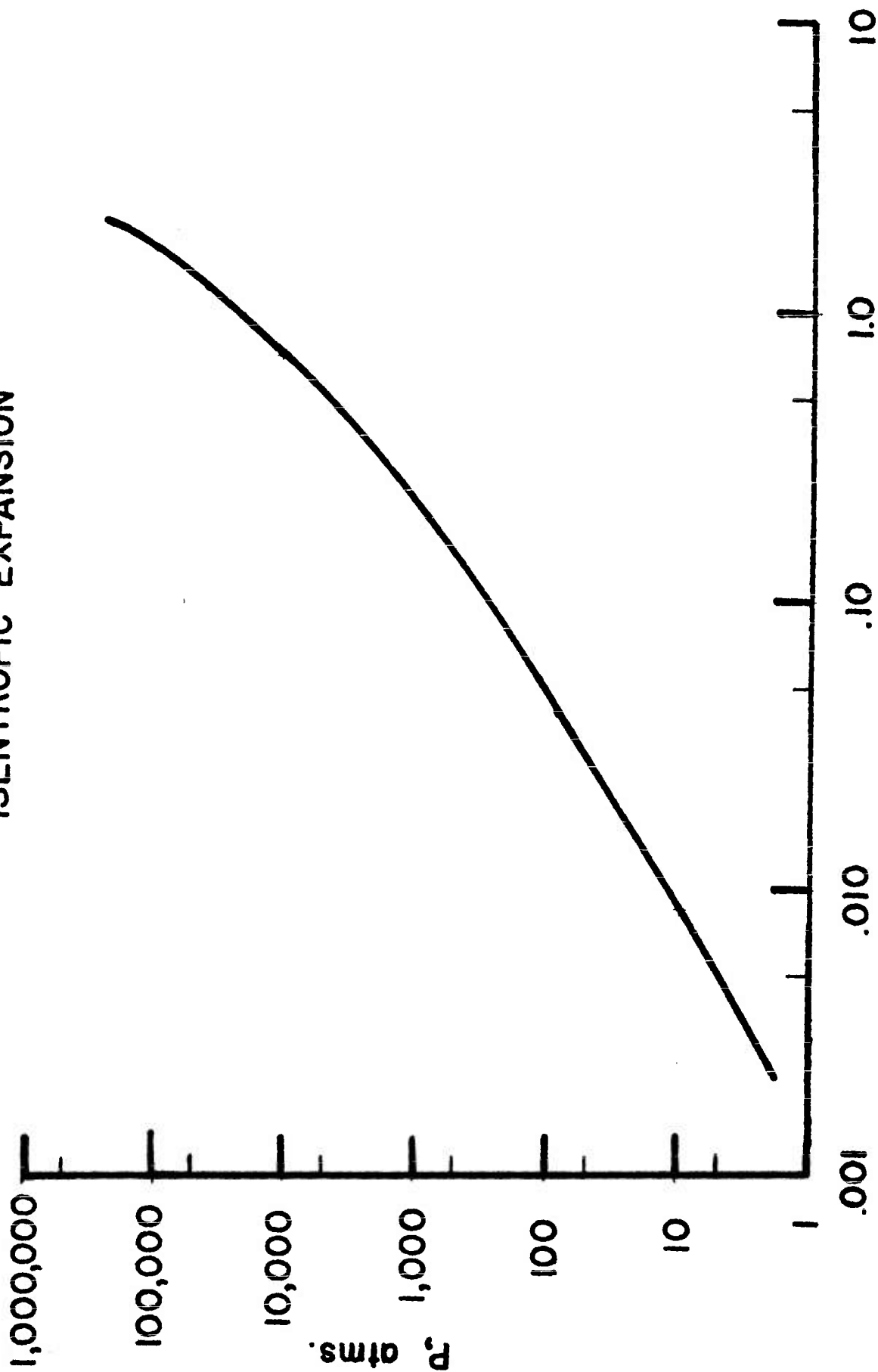
TABLE 8

Flow Properties Behind a Plane Detonation Wave in Pentolite  
At a Loading Density of  $1.65 \text{ g/cm}^3$

$D = 7807 \text{ m/sec}$

$r/R$	$u/D$	$c/D$	$P_{\text{atm}}$	$T^{\circ}\text{K}$
1.0000	.23315	.76685	231350	3367.7
.96096	.21260	.74836	211480	3300
.93071	.19797	.73274	197960	3250
.90004	.18360	.71644	185230	3200
.86890	.16936	.69954	173140	3150
.83740	.15531	.68209	161740	3100
.80543	.14123	.66420	150880	3050
.77349	.12737	.64612	140600	3000
.74147	.11362	.62785	130940	2950
.70965	.09987	.60978	121750	2900
.67813	.08611	.59202	113030	2850
.64908	.07495	.57413	104780	2800
.61449	.05849	.55600	96878	2750
.58265	.04456	.53809	89400	2700
.55092	.03062	.52030	82341	2650
.51942	.01661	.50281	75673	2600
.48797	.00242	.48555	69323	2550
.48262	.00000	.48262	68280	2541.5

# PRESSURE-DENSITY RELATION FOR ISENTROPIC EXPANSION



$\rho$ , gm/cm<sup>3</sup>

FIGURE 1

# VELOCITY DISTRIBUTION BEHIND THE DETONATION WAVE

(PENTOLITE DENSITY 1.65 G/CM<sup>3</sup>)

(D=7807 M/SEC.)

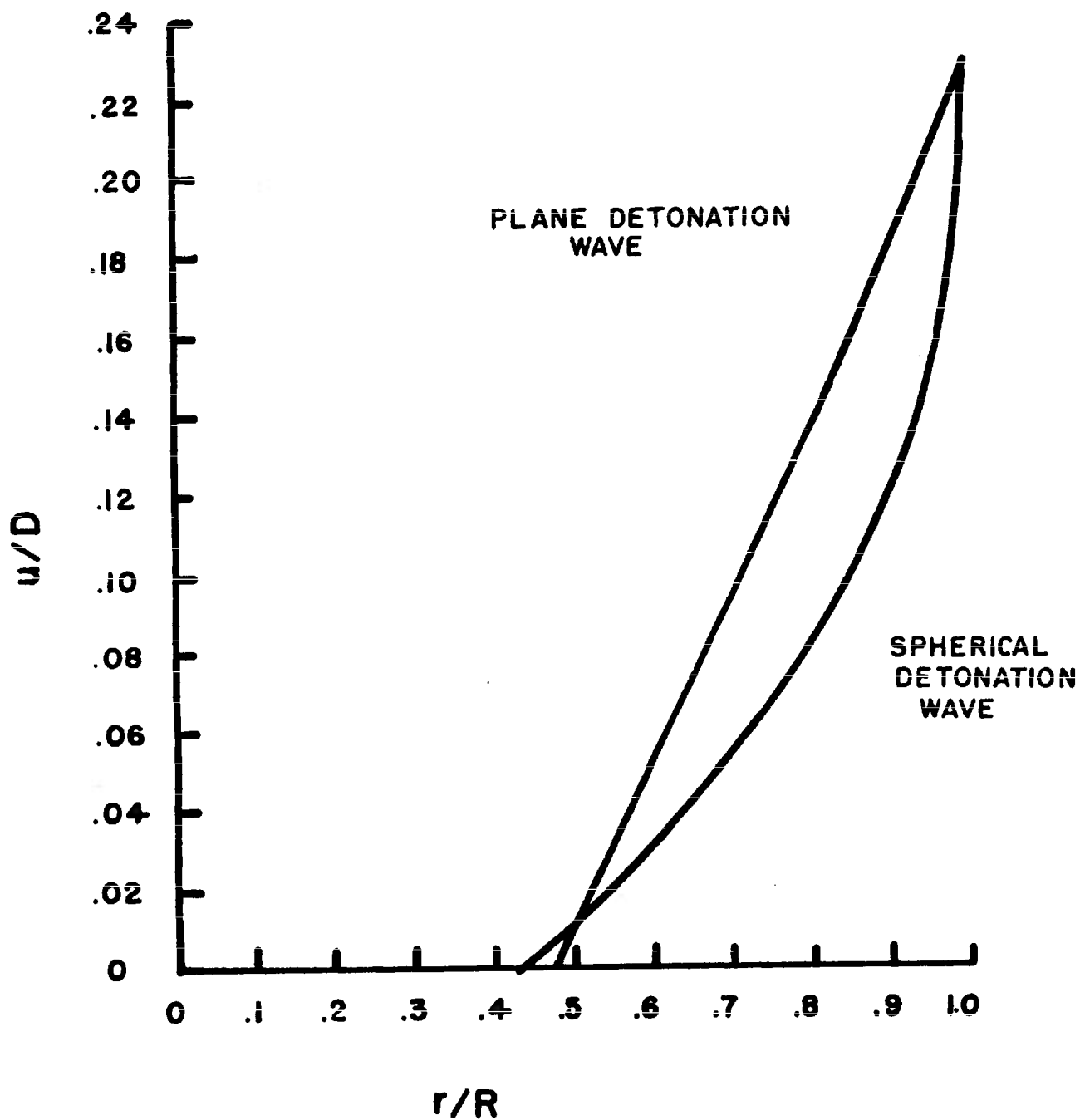


FIGURE 2

# PRESSURE DISTRIBUTION BEHIND THE DETONATION WAVE

(PENTOLITE DENSITY 1.65 G/CM.<sup>3</sup>)

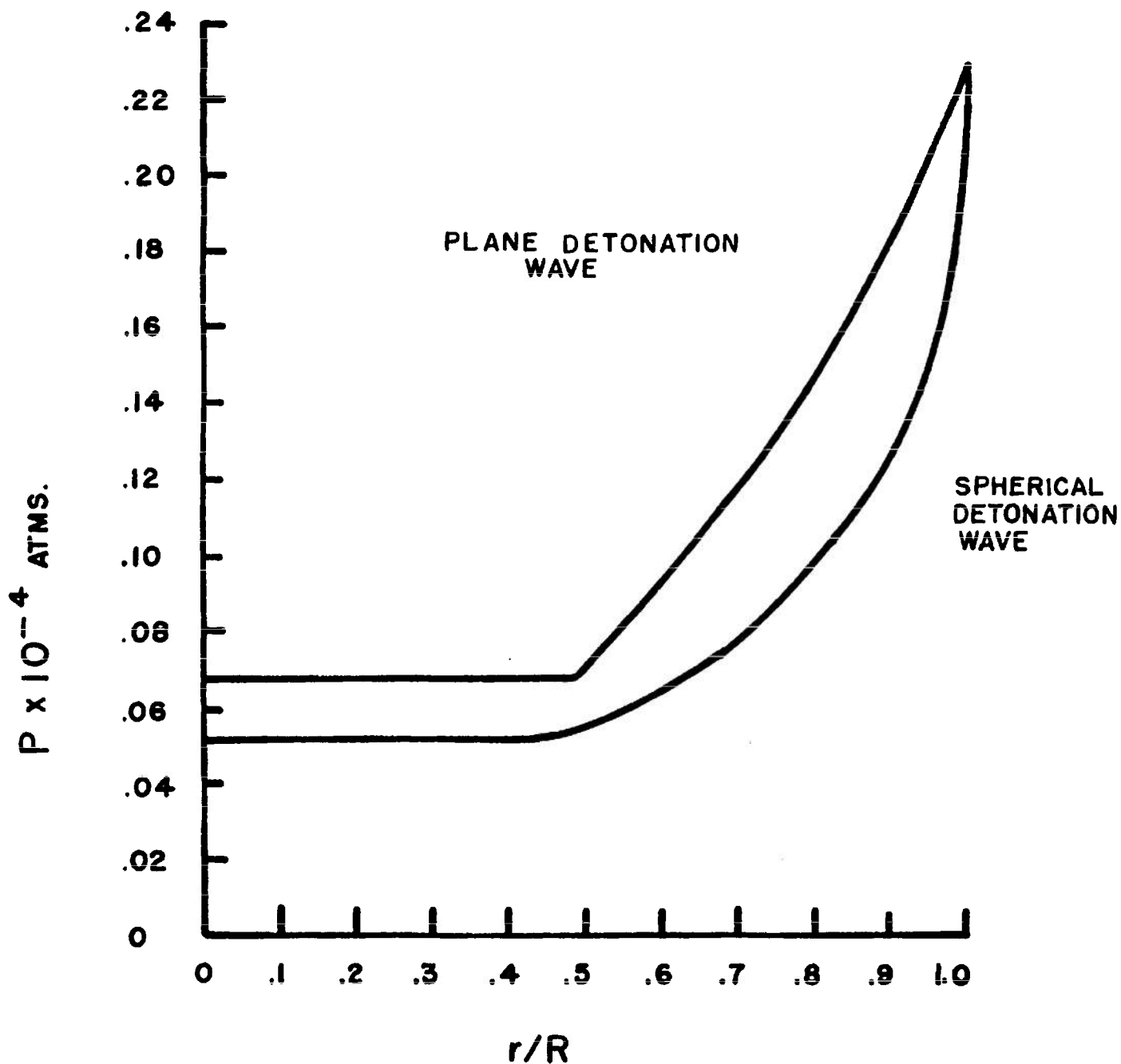


FIGURE 3

# DISTRIBUTION LIST

<u>No. of Copies</u>	<u>Organization</u>	<u>No. of Copies</u>	<u>Organizstion</u>
10	Commander Armed Services Technical Information Agency ATTN: TIPCR Arlington Hall Station Arlington 12, Virginia	2	Commanding General White Sands Missile Range, New Mexico ATTN: Mr. Russell C. Wise - White Sands Annex - BRL ORDBS-OM, Technical Library, RR-10
1	Director of Defense Research and Engineering (OSD) ATTN: Director/Ordnance Washington 25, D.C.	1	Commanding General U.S. Continental Army Command ATTN: CORG - Library Fort Monroe, Virginia
1	Director IDA/Weapon Systems Evaluation Group Room IE880, The Pentagon Washington 25, D.C.	1	Army Research Office Arlington Hall Station Arlington, Virginia
1	Chief of Ordnance ATTN: ORDTB - Bal Sec Department of the Army Washington 25, D.C.	1	Director National Aeronautics and Space Administration 1520 H Street Washington 25, D.C.
1	Commanding General Frankford Arsenal ATTN: Library Branch, 0270, Bldg 40 Philadelphia 37, Pennsylvania	1	Director National Aeronautics and Space Administration ATTN: Mr. Peirce Langley Research Center Langley Field, Virginia
3	Commanding Officer Picatinny Arsenal ATTN: Feltman Research and Engineering Laboratories Dover, New Jersey	1	U.S. Atomic Energy Commission Sandia Corporation Sandia Base Albuquerque, New Mexico
1	Commanding Officer Diamond Ordnance Fuze Laboratories ATTN: Technical Information Office Branch 012 Washington 25, D.C.	4	U.S. Atomic Energy Commission Los Alamos Scientific Laboratory P.O. Box 1663 Los Alamos, New Mexico
1	Research Analysis Corporation ATTN: Document Control Office 6935 Arlington Road Bethesda, Maryland Washington 14, D.C.		



# DISTRIBUTION LIST

<u>No. of Copies</u>	<u>Organization</u>	<u>No. of Copies</u>	<u>Organization</u>
4	University of California Lawrence Radiation Laboratory Technical Information Division ATTN: Clovis G. Craig P.O. Box 808 Livermore, California	2	Commander U.S. Naval Weapons Laboratory Dahlgren, Virginia
	Of Interest to: Mr. Bruce Crowley Dr. Gus Dorough - Chemical Division Dr. Sidney Farnbach Dr. John Foster	2	Commander Air Force Systems Command ATTN: SCRR Andrews Air Force Base Washington 25, D.C.
3	Chief, Bureau of Naval Weapons ATTN: DIS-33 Department of the Navy Washington 25, D.C.	1	Commander Arnold Engineering Development Center ATTN: AEOI Arnold Air Force Station Tullahoma, Tennessee
1	Chief of Naval Operations ATTN: Op 374 - Dr. J. Steinhardt Department of the Navy Washington 25, D.C.	1	Commander Air Force Ballistic Missile Division Headquarters, ARDC ATTN: WDAT Air Force Unit Post Office Los Angeles 45, California
3	Commander Naval Ordnance Laboratory ATTN: Mr. Wm. Filler Mr. Peter Hanlon - Exp. Research Department, Air Ground Exp. Division White Oak, Silver Spring 19, Maryland	1	Commander Air Proving Ground Center ATTN: PGAPI Eglin Air Force Base, Florida  Of Interest to: PGTWR PGTW
2	Commanding Officer Naval Ordnance Laboratory ATTN: Dr. H.A. Thomas Library Corona, California	2	Commander Air Force Cambridge Research Laboratory ATTN: CRRDM - Lt. G. Meltz L.G. Hanscom Field Bedford, Massachusetts
1	Commanding Officer U.S. Naval Air Development Center Johnsville, Pennsylvania	2	Director Air University Library ATTN: AUL (3T-AUL-60-118) Maxwell Air Force Base, Alabama
2	Commander U.S. Naval Ordnance Test Station ATTN: Technical Library China Lake, California	1	Commander Air Force Missile Test Center ATTN: J.R. Atkins - MRSS Patrick Air Force Base, Florida

# DISTRIBUTION LIST

<u>No. of Copies</u>	<u>Organization</u>	<u>No. of Copies</u>	<u>Organization</u>
3	Commander Aeronautical Systems Division ATTN: WWAD WWY WWDS Wright-Patterson Air Force Base, Ohio	1	Armour Research Foundation Illinois Institute of Technology Center ATTN: F. Porzel Chicago 16, Illinois
1	Commander Foreign Technology Division ATTN: Associated Equipment Section, ATIAS Wright-Patterson Air Force Base, Ohio	1	Boeing Airplane Company ATTN: Mr. W.A. Pearce Wichita, Kansas
1	Director, Project RAND Department of the Air Force 1700 Main Street Santa Monica, California	1	Boeing Airplane Company ATTN: Mr. J. Christian - Armament Unit Mr. Ray Elain - Aerospace Division Seattle 24, Washington
5	Chief of Staff U.S. Air Force ATTN: AFDRT AFCOA AFORQ The Pentagon Washington 25, D.C.	1	Broadview Research Corporation ATTN: Mr. Kenneth Kaplan 1811 Trousdale Drive Burlingame, California
1	Director of Research & Development U.S. Air Force ATTN: AFDRT Washington 25, D.C.	1	Chance-Vought Aircraft Company ATTN: Dr. C.C. Wan P.O. Box 5907 Dallas, Texas
1	Aerojet-General Corporation 6352 North Irwindale Road Azusa, California	1	CONVAIR, A Division of General Dynamics Corporation P.O. Box 1950 San Diego 12, California
1	Aerojet-General Corporation Technical Information Office ATTN: R.G. Weitz Sacramento Plants P.O. Box 1947 Sacramento 9, California	1	CONVAIR, A Division of General Dynamics Corporation Fort Worth 1, Texas
2	Aircraft Armaments, Inc. ATTN: Dr. Wilfred Baker Mr. R.R. Mills, Jr. P.O. Box 126 Cockeysville, Maryland	1	Cornell Aeronautical Laboratory, Inc. ATTN: Mr. Joseph Desmond, Librarian Buffalo 5, New York
		1	Douglas Aircraft Company Long Beach, California
		3	General Electric Research Laboratory P.O. Box 1088 Schenectady, New York

# DISTRIBUTION LIST

<u>No. of Copies</u>	<u>Organization</u>	<u>No. of Copies</u>	<u>Organization</u>
1	Grumman Aircraft Engineering Corp. ATTN: Armament Group Bethpage, Long Island, New York	2	The Rand Corporation ATTN: H.L. Brode F.R. Gilmore 1700 Main Street Santa Monica, California
1	Hughes Aircraft Company ATTN: Mr. Dana Johnson Research & Development Labs Florence Avenue at Teale Street Culver City, California	1	Space Technology Laboratories, Inc. ATTN: Technical Information Center Document Processing P.O. Box 95001 Los Angeles 45, California
3	The Martin Company ATTN: Mr. S.L. Rosing Mail No. 356 Middle River, Maryland Mr. Dobray - Mail No. X813 Library Baltimore 3, Maryland	1	Applied Physics Laboratory The Johns Hopkins University 8621 Georgia Avenue Silver Spring, Maryland
1	Lockheed Aircraft Corporation Military Operations Research Division ATTN: Mr. R.A. Bailey - Division Engineer Burbank, California	1	California Institute of Technology Guggenheim Aeronautical Laboratory ATTN: H.W. Leipmann Pasadena, California
1	McDonnell Aircraft Corporation ATTN: Armament Group P.O. Box 516 St. Louis 3, Missouri	1	The Johns Hopkins University Institute for Cooperative Research 3506 Greenway Baltimore 18, Maryland
1	Midwest Research Institute ATTN: B.L. Rhodes 425 Volker Boulevard Kansas City 10, Missouri	2	Massachusetts Institute of Technology ATTN: Dr. James Mar, Bldg 23-111 Dr. Emmett A. Witmer, Rm. 41-219 Cambridge 39, Massachusetts
2	North American Aviation, Inc. ATTN: Mr. D.H. Mason Mr. J. Ward Engineering Technical File 12214 Lakewood Boulevard Downey, California	1	Purdue University Director of Statistical Laboratory ATTN: Dr. Kossach Lafayette, Indiana
1	Northrop Aircraft, Inc. 1001 E. Broadway Hawthorne, California	1	Stanford Research Institute Menlo Park, California
2	Republic Aviation Corporation Farmingdale, Long Island, New York	2	Stevens Institute of Technology Davidson Laboratory ATTN: Dr. S.J. Lukasik Mr. L.H. Weeks Hoboken, New Jersey

# DISTRIBUTION LIST

<u>No. of</u> <u>Copies</u>	<u>Organization</u>	<u>No. of</u> <u>Copies</u>	<u>Organization</u>
1	University of Michigan Department of Engineering ATTN: Dr. O. Laporte Ann Arbor, Michigan	1	Dr. Paul Richards Technical Operations, Inc. Burlington, Massachusetts
1	University of Utah Institute of Rate Processes ATTN: M.A. Cook Salt Lake City, Utah	1	Dr. J.S. Rinehart University of Colorado School of Mines Golden, Colorado
1	Professor W. Bleakney Palmer Physical Laboratory Princeton University Princeton, New Jersey	1	Professor W. Sears Cornell University Graduate School of Aeronautical Engineering Ithaca, New York
1	Dr. S.R. Brinkley Alcoa Building Pittsburgh 19, Pennsylvania	1	Professor G.B. Whitham New York University Institute of Mathematical Sciences 25 Waverly Place New York 3, New York
1	Mr. F.T. Bodurtha E.I. DuPont de Nemours & Company Louviers Building Wilmington 98, Delaware	10	Commander British Army Staff British Defence Staff (W) ATTN: Reports Officer 3100 Massachusetts Avenue, N.W. Washington 8, D.C.
1	Professor J.P. Hirschfelder University of Wisconsin Department of Chemistry Madison, Wisconsin		Of Interest to: Mr. G. Simm R.A.E.
1	Professor K.O. Friedrichs New York University Applied Mathematics Panel New York, New York	4	Defence Research Member Canadian Joint Staff 2450 Massachusetts Avenue, N.W. Washington 25, D.C.
1	Professor M. Holt Brown University Graduate Division of Applied Mathematics Providence 12, Rhode Island		
1	Mr. H.G. Leistner - Civil Engineer Pan American World Airways, Inc. Patrick Air Force Base, Florida		
1	Mr. Robert McAlevy Princeton University Forrestal Research Center Department of Aeronautical Engineering Princeton, New Jersey		

AD Ballistic Research Laboratories, APG DETONATION PROPERTIES OF PENTOLITE Ralph E. Shear	UNCLASSIFIED Pentolite - Detonation Explosives - Theory	AD Ballistic Research Laboratories, APG DETONATION PROPERTIES OF PENTOLITE Ralph E. Shear	UNCLASSIFIED Pentolite - Detonation Explosives - Theory
BRL Report No. 1159 December 1961		BRL Report No. 1159 December 1961	
DA Proj No. 503-04-002, QMSC No. 5010.11.815 UNCLASSIFIED Report		DA Proj No. 503-04-002, QMSC No. 5010.11.815 UNCLASSIFIED Report	
The hydrodynamic theory of detonation has been applied to determine the detonation velocity, pressure, and product composition and the isentropic expansion of the explosion products of pentolite. Hydrodynamic principles were applied to determine the initial pressure of the shock formed in air after completion of the detonation and to calculate the pressure and velocity distribution behind the detonation wave.		The hydrodynamic theory of detonation has been applied to determine the detonation velocity, pressure, and product composition and the isentropic expansion of the explosion products of pentolite. Hydrodynamic principles were applied to determine the initial pressure of the shock formed in air after completion of the detonation and to calculate the pressure and velocity distribution behind the detonation wave.	
AD Ballistic Research Laboratories, APG DETONATION PROPERTIES OF PENTOLITE Ralph E. Shear	UNCLASSIFIED Pentolite - Detonation Explosives - Theory	AD Ballistic Research Laboratories, APG DETONATION PROPERTIES OF PENTOLITE Ralph E. Shear	UNCLASSIFIED Pentolite - Detonation Explosives - Theory
BRL Report No. 1159 December 1961		BRL Report No. 1159 December 1961	
DA Proj No. 503-04-002, QMSC No. 5010.11.815 UNCLASSIFIED Report		DA Proj No. 503-04-002, QMSC No. 5010.11.815 UNCLASSIFIED Report	
The hydrodynamic theory of detonation has been applied to determine the detonation velocity, pressure, and product composition and the isentropic expansion of the explosion products of pentolite. Hydrodynamic principles were applied to determine the initial pressure of the shock formed in air after completion of the detonation and to calculate the pressure and velocity distribution behind the detonation wave.		The hydrodynamic theory of detonation has been applied to determine the detonation velocity, pressure, and product composition and the isentropic expansion of the explosion products of pentolite. Hydrodynamic principles were applied to determine the initial pressure of the shock formed in air after completion of the detonation and to calculate the pressure and velocity distribution behind the detonation wave.	